



# A Novel ANFIS controller for enhanced operation of Wind Turbine based PMSG System during unbalanced Grid Voltage conditions

**Kuragayala Kalyan<sup>1</sup>, Dr.V.Usha Reddy<sup>2</sup>**

<sup>1</sup>M. Tech, Dept. of EEE, SVUCE, Sri Venkateswara University, Tirupati, India

<sup>2</sup>Assistant Professor, Dept. of EEE, SVUCE, Sri Venkateswara University, Tirupati, India

## Abstract

This paper presents a Novel Adaptive Neuro-Fuzzy Inference System (ANFIS) controller for PMSG based Wind Power Generation system (WPGS). The ANFIS controller is employed for power and current limiting control of PMSG-WPGS under unbalance grid voltage conditions. In this proposed scheme, Grid Side Converter (GSC) transmits power to the grid and determines how the Machine Side Converter (MSC) controller regulates the electromagnetic power. In the meantime, it prevents the dc-link from over voltage by converting the unbalanced power into rotor kinetic energy. The three-phase inverter currents should be kept within the converters' safest operating range, and the GSC controller can also meet the grid reactive power whenever it needs. In addition, the GSC controller also used to reduce swings in output power and dc bus voltage. In the controlling topology to regulate the DC link voltage, PI controllers are implemented. But employing PI controllers speed response of the system is less and harmonic distortions are more. To control harmonic distortions and to improve the response of the system a new topology ANFIS is employed in place of PI. The performance of this proposed system is evaluated using MATLAB/Simulink 2018a Software.

**Keywords:** Wind, unbalanced grid, peak current, PMSG, ANFIS controller

## Introduction

The two most important aspects to take into account while managing the existing power system are Wind Turbine Generators (WGs) with regard to Fault Ride through (FRT) and power quality improvement at the grid interface. PMSG-based WGs will make the FRT simple as they are completely decoupled from the grid and power converters [1-3].

The efficiency of these controllers in fulfilling FRT standards is periodically assessed. Grid malfunction results in decrease the grid voltage, which in turn causes a decrease in grid power injection rate. It result an imbalance in the active power flow of the grid integration and capture processes [4].

As wind power is increasingly incorporated into the grid, the dependability and stability of the electricity system are placed at risk. In order to address this issue, grid operators have proposed grid codes to standardize the characteristics of the Wind Energy Conversion System (WECS). The Low Voltage Ride through (LVRT) code, one of the codes, requires that the WECS stay connected and inject the predicted reactive current to support the grid in the event of a grid fault. To achieve this reactive current and standard LVRT profile will be used. While fault time, the WECS should supply reactive currents. Reactive currents should be given at double the proportion for voltage sags lower than 50%. When there is a major fault and the voltage sags are more than 50%, 100% reactive currents are required [5].

Set speed or a Variable speed can be chosen for every WT generator. For instance, Synchronous Generators (SGs) and Doubly-Fed Induction Generators (DFIGs) are commonly used in Variable-Speed Wind Turbines (VSWTs), although Squirrel Cage Induction Generators (SCIGs) can be used in both Fixed-Speed and Variable-Speed Wind Turbines (VSWTs). An overview of potential wind generator systems is also given in addition to comparisons. Despite being simple, dependable and inexpensive. A fixed-speed SCIG-based WECS. High mechanical stress, reactive power load on the power grid, severe power fluctuations, and severely constrained FRT capabilities are some drawbacks of exclusively mechanical systems.

The VSWT can optimize wind power at different wind speeds compared to FSWT, which reduces the mechanical stress on WT by absorbing the changes in wind-power. In this way, the WT's variable-speed operation maximizes its aerodynamic efficiency by producing more power than its fixed-speed operation does [6].

Now a days PMSG technology based on wind turbine are expanding significantly due to improvements in semiconductor switching devices as well as greater dependability and efficiency. Many companies all over the world have lately begun producing 2MW wind turbines based on PMSG.

This work investigates the ANFIS control strategy to regulate the active and reactive power provided into the grid through three-phase voltage source inverter to improve power quality and boost performance under dynamic conditions. The reviewed system is modelled and simulated in MATLAB/SIMULINK. Suggested control ensures that the dc bus voltage is constant without the aid of any external devices and also three-phase peak currents are within safe ranges. Based on the degree of grid voltage sag, reactive power support is provided to the power grid in the meantime. The output power and DC bus voltage can effectively reduced by Grid Side Converter (GSC).

### Problem Statement

As renewable energy becomes more popular over non-renewable energy, the use of alternative power generation methods is growing. Due to this growth, there are increasing complex and changing requirements for controlling those power producing systems. When failures occurs due to imbalance in the grid, conventional regulating methods for these power production systems are unable to demonstrate good controlling outcomes [7–11]. Despite the advantages provided by several controlling approaches in [12-14], certain problems may include less efficient suppression of increased peak current and reactive power variations, over current, over voltage, etc.

A few other approaches similar to grid faults [15–16] were developed over time, but there will always be practical problems. For instance [17] had to create a data table using offline methods, which seemed quite difficult, and helping to raise the voltage of a DC bus. The work of earlier researcher resulted in the suggests[18–20] for reducing the effects of high voltages, but the cost became the main problem in those regulating approaches due to the growing extrinsic devices. These issues were resolved by [21–23], but the controlling was not effective due to asymmetrical defects.

### Objectives of the work

The list of following is to target the main goals:

- To model the grid effectively PMSG based on wind turbine is required.
- Using ANN and FUZZY to create an improved ANFIS controller.
- To manage current and power problems that may arise in case of an imbalanced grid voltage occur in the system.

### Conventional Method

The use of power generators powered by RE- Renewable Energy can significantly reduce emissions of greenhouse gases including CO<sub>2</sub>, CH<sub>4</sub>, and others [24]. This RE adoption could have a number of advantages, such as zero pollution emissions, significantly lower building costs, increased use of generated power, etc. [25]. This has led to more research being done on these advances, as shown by [26] and [27].

Particularly, wind energy could be effectively used to generate electricity by relaying on SCIG- Squirrel Cage Induction Generator, PMSG- Permanent Magnet Synchronous Generators, DFIG- Doubly Fed Induction Generator, etc. to integrate any of them in the utility grid of these generators [28] depending on the need. The problems with those generators increasingly get worse with time due to the wider variety of generators [29-32]. In the literature, numerous works like have been suggested to deal with a variety of power and related concerns. However, there is a need to address the generator problems that arise in unbalanced grid voltage scenarios, which demands the use of cutting-edge controllers.

## II SYSTEM DESCRIPTION

The model of wind power system based on PMSG mainly consists of five parts: GSC, PMSG, MSC, grid, and wind turbine. It can be shown in FIGURE 1.

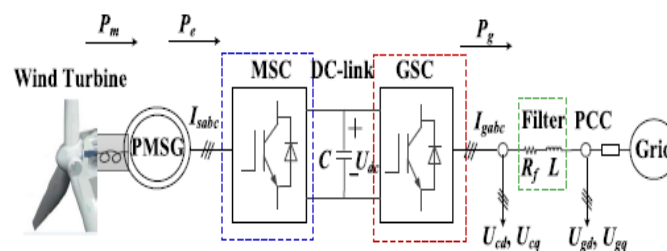


FIGURE 1

## Wind Turbine Modeling

The mechanical power of wind turbine can be obtained by capturing wind, which can be expressed as follows

$$P_m = \frac{1}{2} \pi \rho R^2 C_p(\beta, \lambda) v^3 \quad (1)$$

Here  $\rho$  = Density of air (Kg/m<sup>3</sup>),

R = Radius of blade (m),

$\beta$  = Pitch angle,

$\lambda$  = Tip-speed ratio,

$v$  = Speed of wind (m/s),

Wind energy utilization coefficient denoted as  $C_p$  is calculated by the following formula:

$$\begin{cases} C_p = 0.58(116\lambda_m - 0.4\beta - 5)e^{-21\lambda_m} \\ \lambda_m = \frac{1}{\lambda + 0.008\beta} - \frac{0.0035}{\beta^3 + 1} \\ \lambda = \frac{R\omega_m}{v} \end{cases} \quad (2)$$

Where the mechanical angular velocity is denoted by  $\omega_m$ .

The expression for calculating the mechanical torque experienced by the wind turbine is given below:

$$T_m = \frac{P_m}{\omega_m} = \frac{1}{2} \pi \rho R^3 C_p(\beta, \lambda) V^2 / \lambda \quad (3)$$

## PMSG Modeling

The two-phase rotating d-q coordinate system's voltage equation for the PMSG can be written as

$$\begin{cases} L_{sd} \frac{dI_{sd}}{dt} = -R_s I_{sd} + \omega_e L_{sq} I_{sq} + U_{sd} \\ L_{sq} \frac{dI_{sq}}{dt} = -R_s I_{sq} - \omega_e L_{sd} I_{sd} - \omega_e \psi + U_{sq} \end{cases} \quad (4)$$

Where

$U_{sd}$  = Direct axis voltage

$U_{sq}$  = Quadrature axis voltage

$I_{sd}$  = Direct axis current

$I_{sq}$  = Quadrature axis current

$R_s$  = Stator Resistance ( $\Omega$ )

$L_{sd}$  = Stator inductance on d-axis (mH)

$L_{sq}$  = Stator inductance on q-axis (mH)

$\Psi$  = Permanent magnet chain

$\omega_m$  = Electrical angular speed

The PMSG electromagnetic torque is expressed as

$$T_e = 1.5n_p [(L_{sd} - L_{sq}) I_{sd} I_{sq} + \psi I_{sq}] \quad (5)$$

According to [5], the mechanical characteristics of the system that employs the dynamic one-mass model are as follows:

$$T_m = J \frac{d\omega_m}{dt} + B\omega_m + T_e \quad (6)$$

Here J = Transmission system's moment of inertia

B = Transmission system's self-damping coefficient

## Grid Modeling

Since there is no circulation path of zero sequence component in three-phase three-wire system, zero sequence component is not considered. Using the DSC (Delayed Signal Cancellation) approach, the three-phase unbalanced voltages can be separated into positive sequence and negative sequence voltage parts. The imbalanced voltages could be expressed as

$$[U_{ga}U_{gb}U_{gc}]^T = \begin{bmatrix} U^+ \sin(\omega t + \theta^+) + U^- \sin(\omega t + \theta^-) \\ U^+ \sin(120^\circ + \theta^+) + U^- \sin(\omega t + 120^\circ + \theta^-) \\ U^+ \sin(\omega t + 120^\circ + \theta^+) + U^- \sin(\omega t - 120^\circ + \theta^-) \end{bmatrix} \tag{7}$$

Here  $U^+$  = Voltage amplitude of positive sequence element

$\theta^+$  = Initial phase of the positive sequence element

$U^-$  = Voltage amplitude of negative sequence element

$\theta^-$  = Initial phase of the negative sequence element

$\omega$  = Grid voltage's angle frequency

By using Clark transformation three-phase voltages can be converted into stationary coordinate system, Which can be expressed as

$$\begin{bmatrix} U_{g\alpha} \\ U_{g\beta} \end{bmatrix} = \frac{2}{3} \begin{bmatrix} 1 & -\frac{1}{2} & -\frac{1}{2} \\ 0 & \frac{\sqrt{3}}{2} & -\frac{\sqrt{3}}{2} \end{bmatrix} \begin{bmatrix} U_{ga} \\ U_{gb} \\ U_{gc} \end{bmatrix} = \begin{bmatrix} U^+_{g\alpha} + U^-_{g\beta} \\ U^+_{g\beta} + U^-_{g\beta} \end{bmatrix} \tag{8}$$

$$\begin{bmatrix} U^+_{g\alpha} \\ U^+_{g\beta} \\ U^-_{g\alpha} \\ U^-_{g\beta} \end{bmatrix} = \begin{bmatrix} U^+ \sin(\omega t + \theta^+) \\ -U^+ \cos(\omega t + \theta^+) \\ U^- \sin(\omega t + \theta^-) \\ U^- \cos(\omega t + \theta^-) \end{bmatrix} \tag{9}$$

Where  $U^+_{g\alpha}, U^+_{g\beta}$ , and  $U^-_{g\alpha}, U^-_{g\beta}$  represent, respectively, the positive and negative sequence voltage elements.

Following are the active and reactive power outputs according to instantaneous power theory.

$$\begin{bmatrix} P_g \\ Q_g \end{bmatrix} = \frac{3}{2} \begin{bmatrix} U_{g\alpha} & U_{g\beta} \\ U_{g\beta} & -U_{g\alpha} \end{bmatrix} \begin{bmatrix} I_\alpha \\ I_\beta \end{bmatrix} \tag{10}$$

### III PROPOSED ANFIS-BASED CONTROLLER

Use of ANFIS control instead of conventional PI controller can be an effective way to solve the problem of system parameters change. Hence, a good control performance can be achieved. Therefore, application of ANFIS controller on the PMSG converter controller system is proposed in this paper. The ANFIS controller has advantages of robust, simple, and easy to be modified.

To create the innovative controller, an ANFIS-Adaptive Neuro-Fuzzy Inference System on Takagi-Sugeno fuzzy inference system and artificial neural network technology. Because it incorporates both of these ideas, it has the ability to combine the benefits of neural networks and fuzzy logic in a single framework and perform effectively by managing both current and power even in the case of an imbalanced grid voltage.

Inference system is based on a set of fuzzy IF-THEN rules that can learn and approximatively represent non-linear functions. The IF-THEN-ELSE rule and the use of linguistic concepts make fuzzy rule bases easy to comprehend. Fuzzy logic, unlike neural networks, cannot learn on its own. Neural networks can learn from data. Understanding the knowledge that neural networks have collected has proved difficult.

The ANFIS neural network methodology is a data-driven strategy. A clustered training set of numerical samples forms the basis of the ANFIS synthesis technique.

In this study ANFIS is trained from the input and output data generated from proportional and integral controllers (q-axis current controller and d-axis current controller). The inputs to ANFIS are the error and error changer. The output of ANFIS are reference stator voltages and that are used as input signals for the space vector block to control of Grid Side converter.

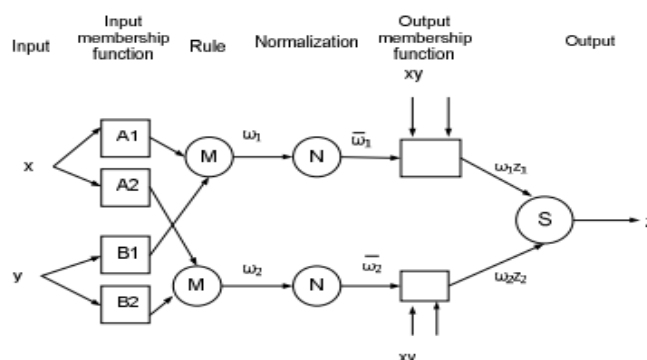


Figure 2. ANFIS structure

Parameters	Value
Rated Capacity[MW]	1.5
Air density $\rho$ [kg/m <sup>3</sup> ]	1.225
Wind wheel radius $R$ [m]	31
Maximum wind energy utilization coefficient $C_{p\_max}$	0.476
Rated wind speed $v_{rate}$ [m/s]	12
Pole logarithm of PMSG	102
Magnitude of permanent magnet flux of rotor [Wb]	1.25
Stator resistance $R_s$ [ $\Omega$ ]	0.001
Stator inductance on d-axis $L_d$ [mH]	0.835
Stator inductance on q-axis $L_q$ [mH]	0.835
Rated grid voltage $U$ [V]	690
Bus voltage $U_{dc}$ [V]	1800
DC side filter resistance $R_f$ [ $\Omega$ ]	0.001
DC side filter inductor $L$ [mH]	6
DC side filter capacitor $C$ [F]	2.2
Line impedance $Z$ [ $\Omega$ ]	1+j0.01
Switching frequency $f_{sw}$ [kHz]	10
Sampling period $T_s$ [ $\mu$ s]	100

Table 1. System Parameters

#### IV SIMULATION & RESULTS

Many simulation analysis and results using the MAT-LAB/SIMULINK to evaluate the control performance of the system are presented in this section.

##### Simulation results by deploying PI controller

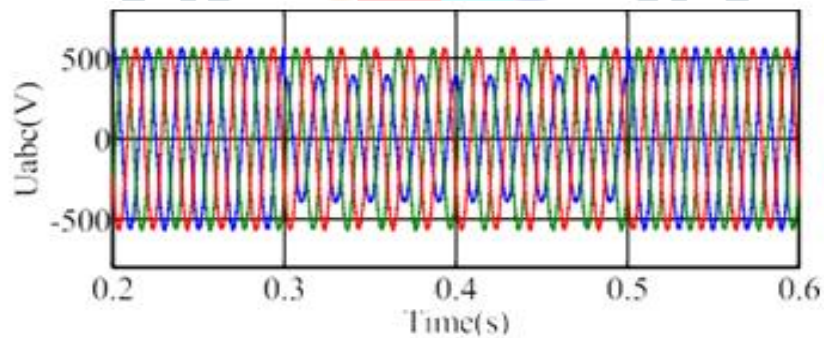


Figure 3(a). The 3 phase unbalanced voltage with  $395\angle 90^\circ$ ,  $563\angle -30^\circ$ ,  $563\angle -150^\circ$  under case 1

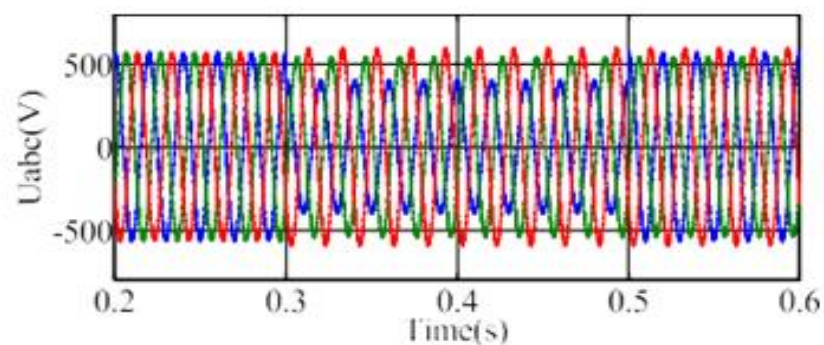
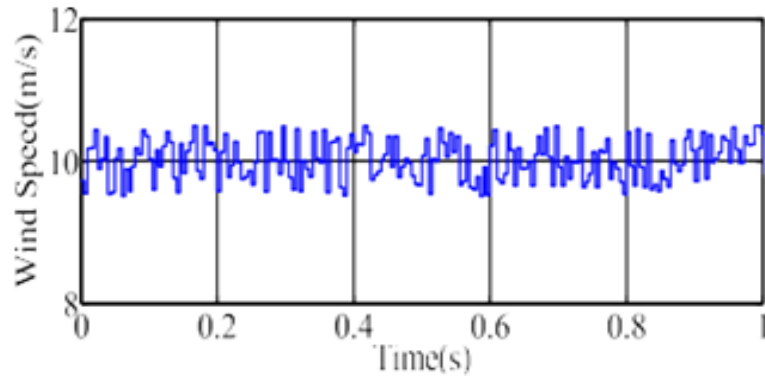
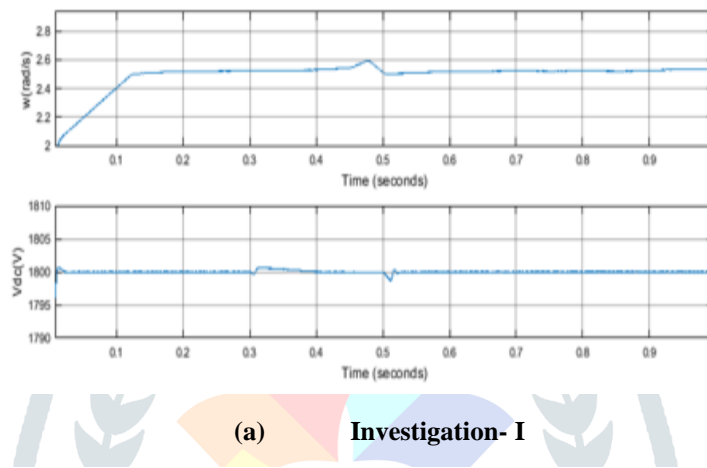


Figure 3(b). The 3 phase unbalanced voltage with  $395\angle 86^\circ$ ,  $540\angle -28^\circ$ ,  $588\angle -148^\circ$  under case 2

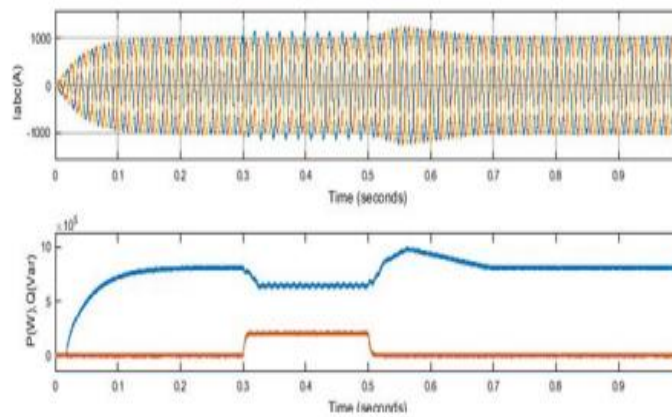


**Figure 4. Depiction of Uniform speed of Wind**

Figures 3a, 3b and 4 above illustrate three-phase unbalanced voltages and wind speed under 30% of voltage sag for the duration of 0.3 to 0.5 seconds. PI controller is used to maintain wind speed under this scenario.



**(a) Investigation- I**



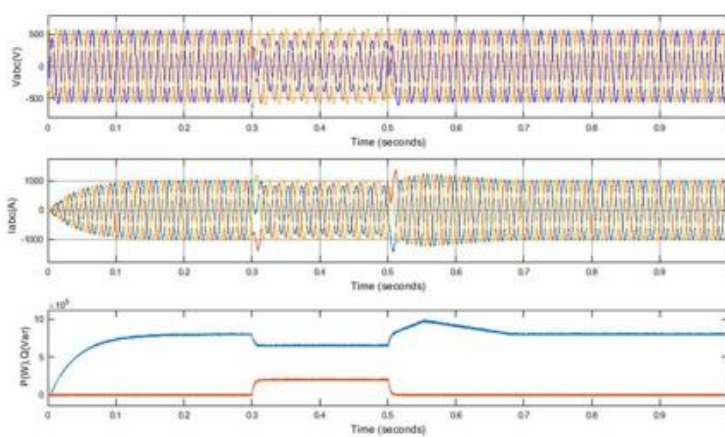
**(b) Investigation- II**



(c) Investigation- III

**Figure 5. Investigations of performance of Control imparted by PI Controller for case 1**

Figure 5 above displays the outcomes of case 1's control strategies. Voltage sag effects are not properly taken into account during the control scheme design. Because of this, utilizing a PI controller causes significant variations in both the output power and dc bus voltage.



(a) Investigation- I



(b) Investigation- II

**Figure 6. Investigations of performance of Control imparted by PI Controller for case 2**

Figure 6 above shows the control results of several control strategies for the second example. Figure 6 illustrates the control results obtained by using the control technique (a). The output current reaches a high value by exceeding the typical value at the time of the grid voltage sag, whereas the output power fluctuations are clearly quite large. Figure 6 shows the control outcomes of the control technique (b). The peak value of the inverter current is greater than the usual operating value despite being lower than that of the control

scheme, and the peak value of the dc bus voltage is unusually high. Additionally, there are still variations in reactive power. The suggested control schema's control results are clearly displayed. The output power fluctuations are eliminated, and the maximum output current is significantly reduced.

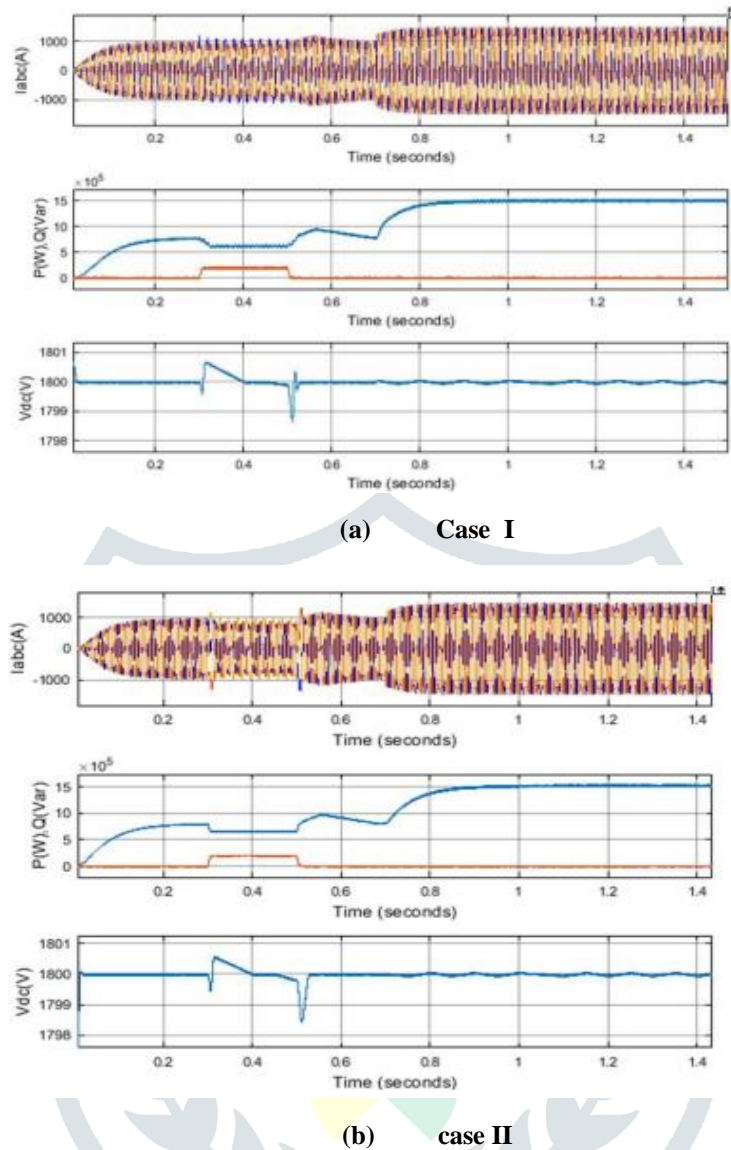
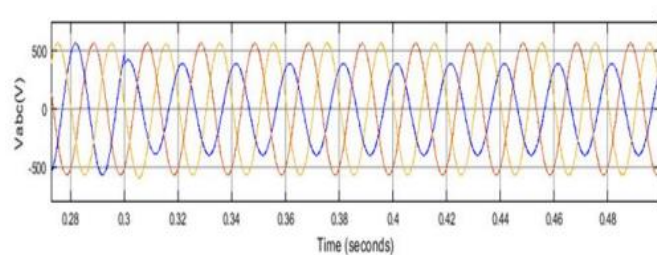
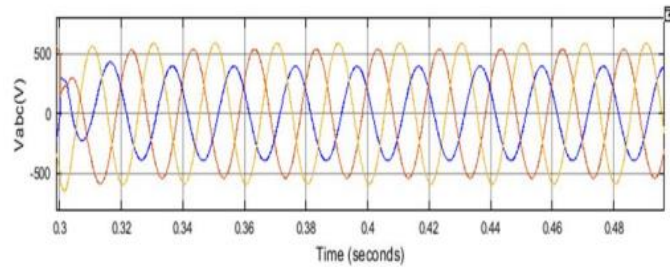


**Figure 7. Investigation of control effect with wind speed step Change with regards to two fault iterations by PI controller**

Figure 7 shows the control outcomes under 2 faults in the unique grid of the asymmetrical nature in order to demonstrate the system's capacity to react dynamically to variations in wind speed. The power of the system also changes from 0.8 MW to 1.5 MW and also wind speed changes from 10 m/s to 12 m/s in 0.7 seconds. Inversely, the DC bus voltage is always steady, and the bus voltage variation range during the transient process is not more than 0.05%. Additionally, it is important to take the system variables quickly and respond to step changes in wind speed when utilizing a PI controller.



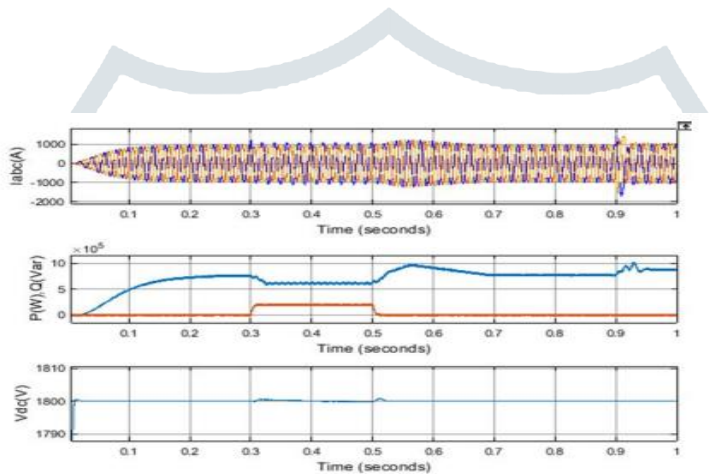
**(a) case I**



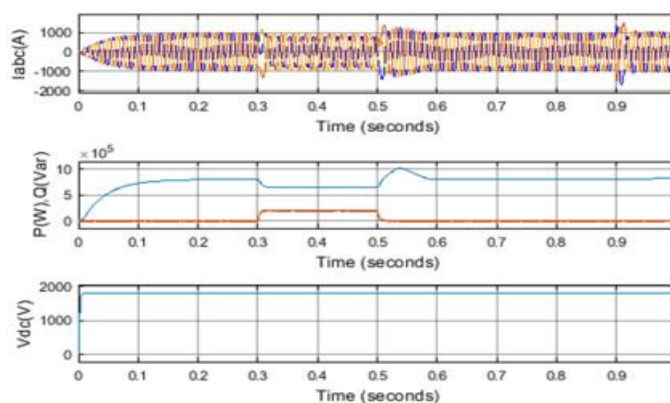
(b) case II

**Figure 8. 3-Phase Voltage in the Grid with regards to two fault iterations by PI controller**

Figure 8 shows the control outcomes for favorable grid assistance using the suggested control strategy for imbalanced grid voltage. The voltage of the PCC for example is also shown in the figure. Take phase a voltage as an example. Figure 8(b) presents the voltage of PCC in case b, the phase a voltage increased from 395 V to 403 V. Which is used to facilitate the grid voltage restores. It is verified that the control strategy can support the power grid according to sag degree of unbalanced voltage, which is contribute to raise the voltage.



(a) Case I



(b) case II

**Figure 9. Investigation of control effect during the change of inductance with regards to two fault iterations by PI controller**

The above figure 9 shows results for control scheme of voltage of dc link, reactive and active power, and three phase currents when inductance changes by using PI controller.

Simulation results by using ANFIS controller

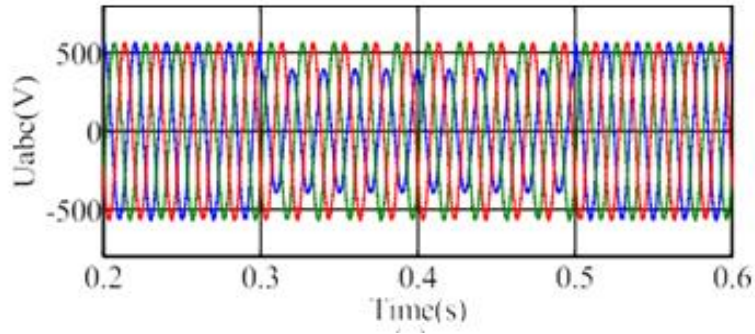


Figure 10(a). The 3 phase unbalanced voltage with  $395\angle 90^\circ, 563\angle -30^\circ, 563\angle -150^\circ$  under case 1

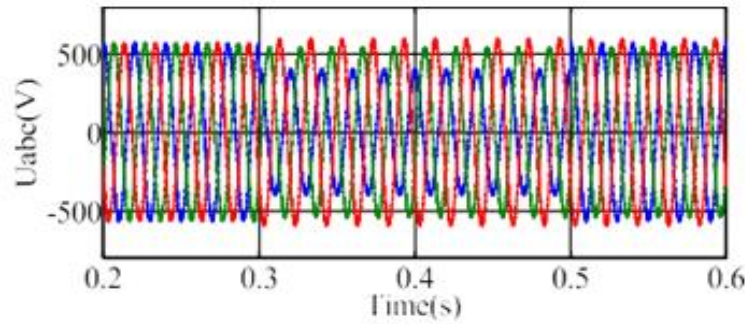


Figure 10(b). The 3 phase unbalanced voltage with  $395\angle 86^\circ, 540\angle -28^\circ, 588\angle -148^\circ$  under case 2

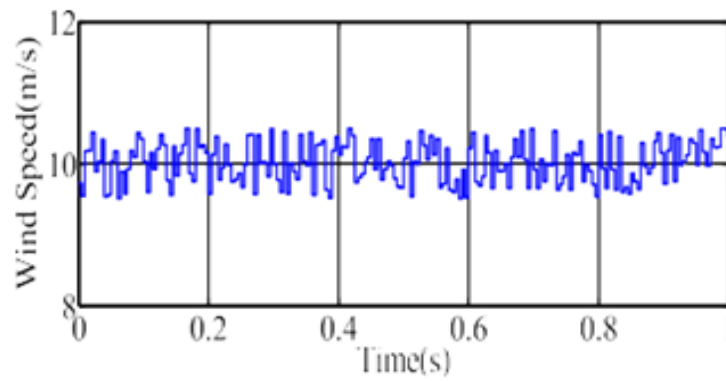
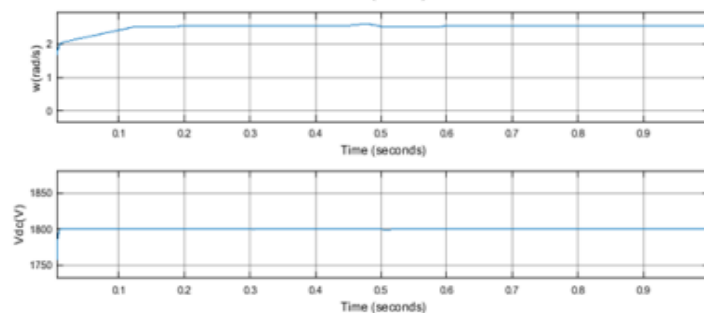
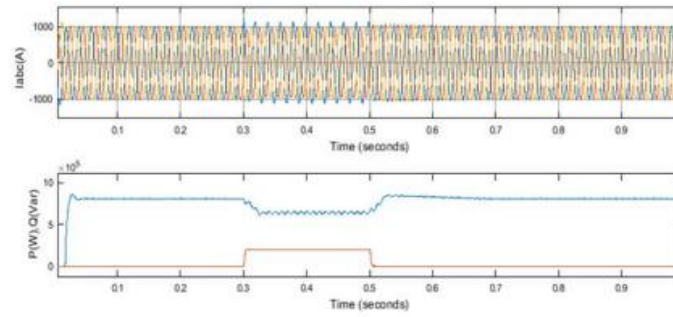


Figure 11. Depiction of Uniform speed of Wind

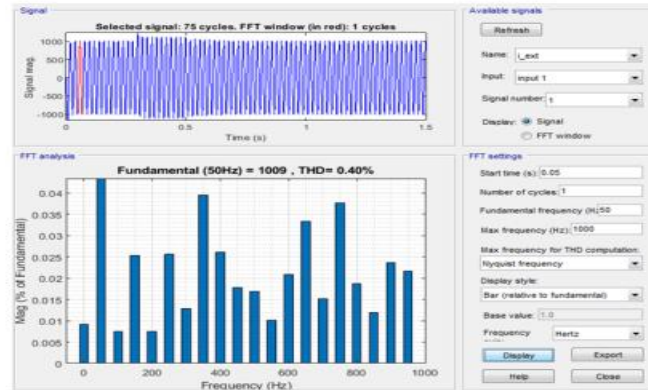
The figure 10 and 11 show three-phase unbalanced voltages and wind speed under 30% of voltage sag during the period from 0.3 to 0.5sec, the wind speed is constant during this condition by using ANFIS controller.



(a) case I



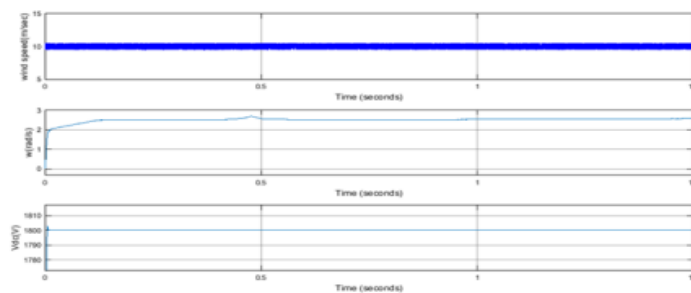
(b) case II



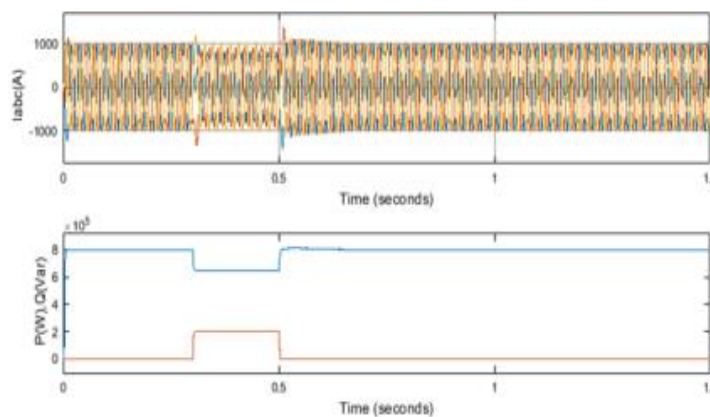
(c) case III

Figure 12. Analysis of performance of Control imparted for case 1

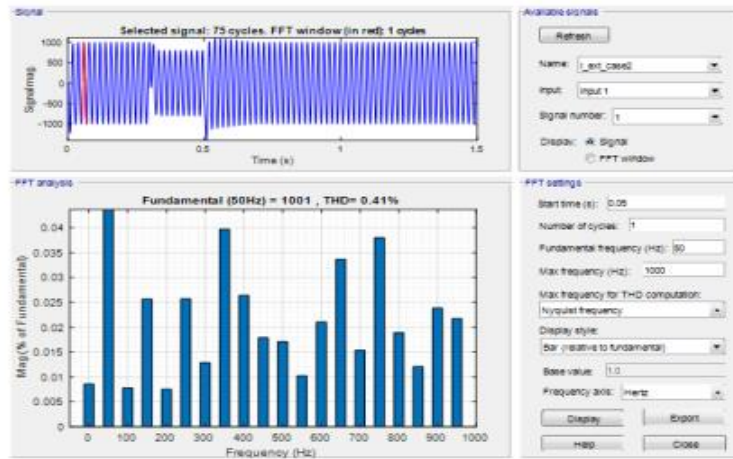
The above figure 12 shows control results using control schemes under case 1. The control scheme design does not fully account for the impact of voltage sag. As a result, there are large fluctuations in both the output power and dc bus voltage by using ANFIS controller



(a) case I



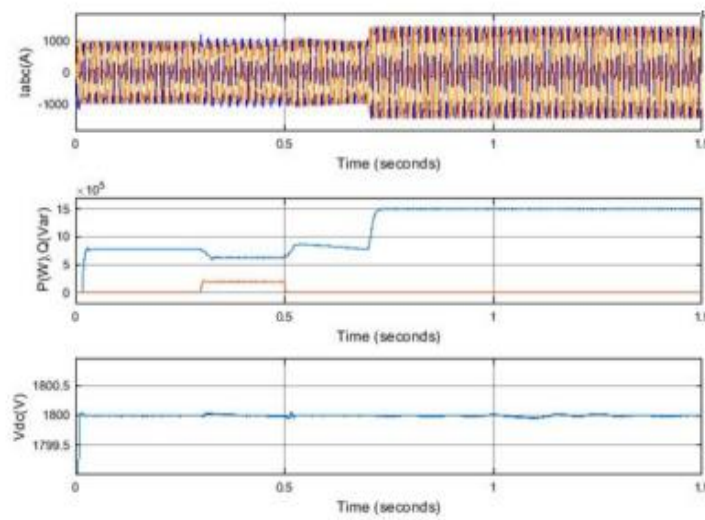
(b) case II



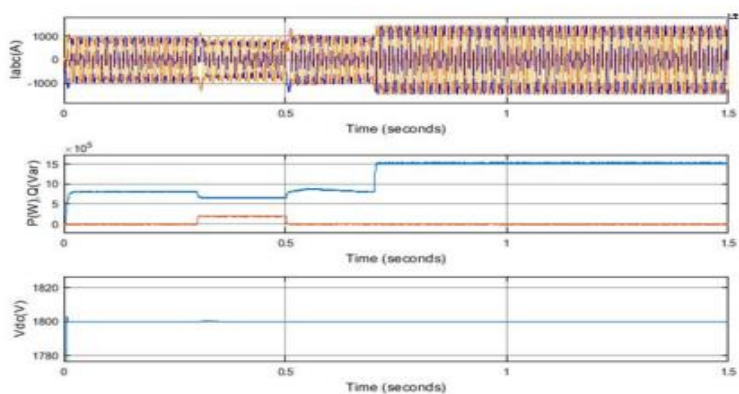
(c) Case III

**Figure 13. Investigations of performance of Control imparted by ANFIS Controller for case 2**

The above figure 13 shows results for control scheme of voltage of dc link, reactive and active power, and three phase currents when inductance changes by using ANFIS controller.



(a) Case I



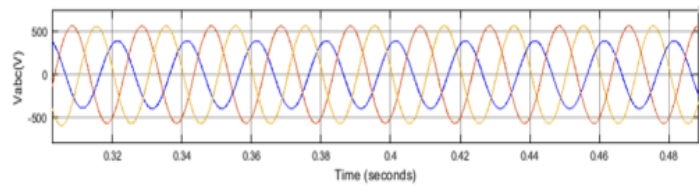
(b) case II

**Figure 14. Investigation of control effect with wind speed step change with regards to two fault iterations by ANFIS controller**

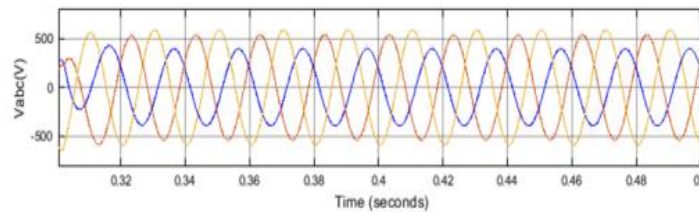
The control outcomes under 2 faults in the separate asymmetrical grid are shown in figure 14 to demonstrate the system's capacity to react dynamically to variations in wind speed. The power of the system increases from 0.8 MW to 1.5 MW as the wind speed increases from 10 m/s to 12 m/s in 0.7 seconds. Contrarily, the dc bus voltage is always steady, and the bus voltage variation range during the

transient process is no more than 0.05%. Furthermore, it is important to take into account the system variables' ability to quickly settle and respond to step changes in wind speed while utilising the ANFIS controller.

**Investigation of 3-Phase Voltage in the Grid**



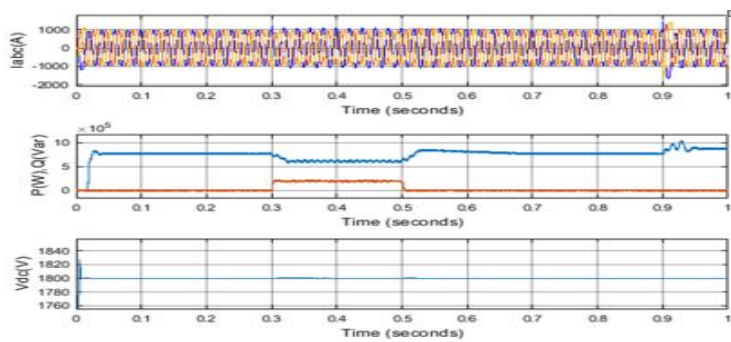
(a) case I



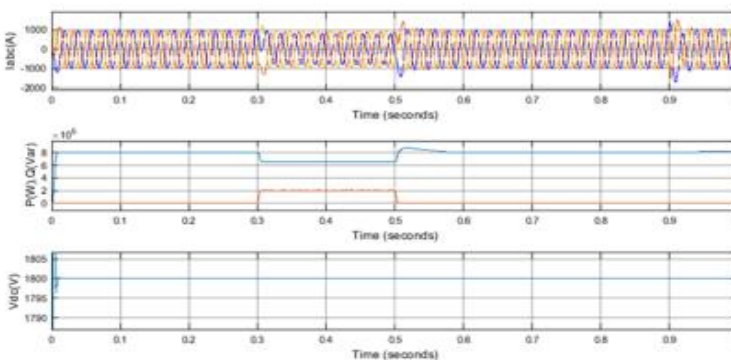
(b) case II

**Figure 15. Investigation of 3-Phase Voltage in the Grid with regards to two fault iterations by ANFIS controller**

The control outcomes of friendly grid support using the suggested control strategy are shown in FIGURE 8 for unbalanced grid voltage, which have been shown in the above figure 15.



(a) case I



(b) case II

**Figure 16. Investigation of control effect during the change of inductance with regards to two fault iterations by ANFIS controller**

The above figure 16 shows results for control scheme of voltage of dc link, reactive and active power, and three phase currents when inductance changes by using ANFIS controller.

## V CONCLUSION

In order to improve operation performance under unbalanced grid voltage, this study introduces a new ANFIS controller for power and current limiting control of wind turbine based on PMSG. The proposed ANFIS controller ensures that the dc bus voltage is steady without the need of any external devices and also three-phase peak currents are within acceptable limits. According to the degree of grid voltage sag, reactive power support is given for the electrical grid in the meantime. The entire proposed scheme is implemented in MATLAB/SIMULINK 2018a software. Comparing the simulation results with the other two control strategies under the two different grid faults has proven the effectiveness and superiority of proposed ANFIS

## VI REFERENCES

- [1] W. Rui, S. Qiuye, M. Dazhong, and H. Xuguang, "Line impedance cooperative stability region identification method for grid-tied inverters under weak grids," *IEEE Trans. Smart Grid*, vol. 11, no. 4, pp. 2856–2866, Jul. 2020.
- [2] R. Vijayapriya, P. Raja, and M. P. Selvan, "A modified active power control scheme for enhanced operation of PMSG-based WGs," *IEEE Trans. Sustain. Energy*, vol. 9, no. 2, pp. 630–638, Apr. 2018.
- [3] H. Geng, L. Liu, and R. Li, "Synchronization and reactive current support of PMSG-based wind farm during severe grid fault," *IEEE Trans. Sustain. Energy*, vol. 9, no. 4, pp. 1596–1604, Oct. 2018.
- [4] J. Tian, J. Liu, J. Shu, J. Tang, and J. Yang, "Engineering modelling of wind turbine applied in real-time simulation with hardware-in-loop and optimising control," *IET Power Electron.*, vol. 11, no. 15, pp. 2490–2498, Nov. 2018.
- [5] H. D. Tafti, A. I. Maswood, G. Konstantinou, J. Pou, and P. Acuna, "Active/reactive power control of photovoltaic grid-tied inverters with peak current limitation and zero active power oscillation during unbalanced voltage sags," *IET Power Electron.*, vol. 11, no. 6, pp. 1066–1073, May 2018.
- [6] M. Nasiri and R. Mohammadi, "Peak current limitation for grid side inverter by limited active power in PMSG-based wind turbines during different grid faults," *IEEE Trans. Sustain. Energy*, vol. 8, no. 1, pp. 3–12, Jan. 2017.
- [7] X. Guo, W. Liu, and Z. Lu, "Flexible power regulation and current limited control of the grid-connected inverter under unbalanced grid voltage faults," *IEEE Trans. Ind. Electron.*, vol. 64, no. 9, pp. 7425–7432, Sep. 2017.
- [8] M. Nasiri, J. Milimonfared, and S. H. Fathi, "A review of low-voltage ride-through enhancement methods for permanent magnet synchronous generator based wind turbines," *Renew. Sustain. Energy Rev.*, vol. 47, pp. 399–415, Jul. 2015.
- [9] M. A. A. Rani, C. Nagamani, G. Saravanallango, and A. Karthikeyan, "An effective reference generation scheme for DFIG with unbalanced grid voltage," *IEEE Trans. Sustain. Energy*, vol. 5, no. 3, pp. 1010–1018, Jul. 2014.
- [10] C. Wessels, N. Hoffmann, M. Molinas, and F. W. Fuchs, "StatCom control at wind farms with fixed-speed induction generators under asymmetrical grid faults," *IEEE Trans. Ind. Electron.*, vol. 60, no. 7, pp. 2864–2873, Jul. 2013.
- [11] S. Li, T. A. Haskew, R. P. Swatloski, and W. Gathings, "Optimal and direct current vector control of direct-driven PMSG wind turbines," *IEEE Trans. Power Electron.*, vol. 27, no. 5, pp. 2325–2337, May 2012.
- [12] J. Miret, M. Castilla, A. Camacho, L. G. D. Vicuña, and J. Matas, "Control scheme for photovoltaic three-phase inverters to minimize peak currents during unbalanced grid-voltage sags," *IEEE Trans. Power Electron.*, vol. 27, no. 10, pp. 4262–4271, Oct. 2012.
- [13] N. Mohan, Dr V. Usha Reddy, "Design and analysis of fractional order PID control for three phase standalone Hybrid PV-Wind Generation", *Muktshabd Journal, Impact Factor*. Volume 10, Issue 3, pp-828-839, March 2021.
- [14] S. Li, T. A. Haskew, and Y. Hong, "PMSG maximum wind power extraction control using adaptive virtual lookup table approach in direct-current vector control structure," *Int. J. Energy Res.*, vol. 35, no. 11, pp. 929–1022, Sep. 2011.
- [15] S. Li, T. A. Haskew, and L. Xu, "Control of HVDC light systems using conventional and direct-current vector control approaches," *IEEE Trans. Power Electron.*, vol. 25, no. 12, pp. 3106–3118, Dec. 2010.
- [16] M. Castilla, J. Miret, J. L. Sosa, J. Matas, and L. G. de Vicuña, "Grid fault control scheme for three-phase photovoltaic inverters with adjustable power quality characteristics," *IEEE Trans. Power Electron.*, vol. 25, no. 12, pp. 2930–2940, Dec. 2010.
- [17] S. Li, T. A. Haskew, and L. Xu, "Conventional and novel control designs for direct driven PMSG wind turbines," *Electr. Power Syst. Res.*, vol. 80, no. 3, pp. 328–338, Mar. 2010.
- [18] M. E. Haque, M. Negnevitsky, and K. M. Muttaqi, "A Novel Control Strategy for a Variable-Speed Wind Turbine With a Permanent-Magnet Synchronous Generator," *IEEE Transactions on Industry Applications*, vol. 46, pp. 331–339, 2010.
- [19] Z. Chen, J. M. Guerrero, and F. Blaabjerg, "A review of the state of the art of power electronics for wind turbines," *IEEE Trans. Power Electron.*, vol. 24, no. 8, pp. 1859–1875, Aug. 2009.
- [20] W. Qiao, L. Qu, and R. G. Harley, "Control of IPM synchronous generator for maximum wind power generation considering magnetic saturation," *IEEE Trans. Ind. Appl.*, vol. 45, no. 3, pp. 1095–1105, Jun. 2009.
- [21] F. Velenciaga and P. F. Puleston, "High-order sliding control for a wind energy conversion system based on a permanent magnet synchronous generator," *IEEE Trans. Energy Convers.*, vol. 23, no. 3, pp. 860–867, Sep. 2008.

- [22] J. Matas, M. Castilla, J. M. Guerrero, L. Garcia de Vicuna, and J. Miret, "Feedback linearization of direct-drive synchronous wind-turbines via a sliding mode approach," *IEEE Trans. Power Electron.*, vol. 23, no. 3, pp. 1093–1103, May 2008.
- [23] D. Santos-Martin, J. L. Rodriguez-Amenedo, and S. Arnalte, "Direct power control applied to doubly fed induction generator under unbalanced grid voltage conditions," *IEEE Trans. Power Electron.*, vol. 23, no. 5, pp. 2328–2336, Sep. 2008.
- [24] P. Rodriguez, A. V. Timbus, R. Teodorescu, M. Liserre, and F. Blaabjerg, "Flexible active power control of distributed power generation systems during grid faults," *IEEE Trans. Ind. Electron.*, vol. 54, no. 5, pp. 2583–2592, Oct. 2007.
- [25] J. Belhadj and X. Roboam, "Investigation of different methods to control a small variable-speed wind turbine with PMSM drives," *J. Energy Resources Technol.*, vol. 129, pp. 200–213, Sep. 2007.
- [26] Y. Suh and T. A. Lipo, "Control scheme in hybrid synchronous stationary frame for PWM AC/DC converter under generalized unbalanced operating conditions," *IEEE Trans. Ind. Appl.*, vol. 42, no. 3, pp. 825–835, Jun. 2006.
- [27] M. Chinchilla, S. Arnalte, and J. C. Burgos, "Control of permanent magnet generators applied to variable-speed wind-energy systems connected to the grid," *IEEE Trans. Energy Convers.*, vol. 21, no. 1, pp. 130–135, Mar. 2006.
- [28] R. Zavadil, N. Miller, A. Ellis, and E. Muljadi, "Making connections: Wind generation challenges and progress," *IEEE Power Energy Mag.*, vol. 3, no. 6, pp. 26–37, Nov. 2005.
- [29] Y. Chen, P. Pillary, and A. Khan, "PM wind generator topologies," *IEEE Trans. Ind. Appl.*, vol. 41, no. 6, pp. 1619–1626, Nov./Dec. 2005.
- [30] K. Tan and S. Islam, "Optimum control strategies in energy conversion of PMSG wind turbine system without mechanical sensors," *IEEE Trans. Energy Convers.*, vol. 19, no. 2, pp. 392–399, Jun. 2004.
- [31] A. D. Hansen, P. Sørensen, F. Iov, and F. Blaabjerg, "Control of variable speed wind turbines with doubly-fed induction generators," *Wind Eng.*, vol. 28, no. 4, pp. 411–432, Jun. 2004.
- [32] M. A. Soliman et al., "Hybrid ANFIS-GA-based control scheme for performance enhancement of a grid-connected wind generator", *IET Renew. Power Gener.*, vol. 12, no. 7, pp. 832-843, 2018.

